Study of Structural, Morphological and Optical, Properties of Fe Doped SnO$_2$ Semiconductor Thin Films Prepared by Sol-Gel Technique

S. Benkara[1(✉)], H. Ghamri[2], and M. Zaabat[3]

[1] Electrical Engineering Department, Larbi Ben M'hidi University, Oum El Bouaghi, Algeria
salimabenkara@gmail.com
[2] Physic Department Hadj Lakhder University, Batna, Algeria
[3] Laboratory of Active Components and Materials,
Oum El Bouaghi University, Oum El Bouaghi, Algeria

Abstract. The undoped and iron doped tin oxide thin films were deposited on glass substrates by sol-gel dip coating technique, using tin chloride and iron III chloride as the starting materials. The effect of method conditions and Fe doping on the structural, morphological and optical properties of applied thin films have been studied by X-ray diffraction (XRD), and UV–vis spectroscopy. Surface topography of thin films was examined by atomic force microscopy (AFM).

XRD patterns showed an increase in peak intensities of the rutile and cubic crystalline phases of SnO$_2$ by increasing the Fe content. SnO$_2$ nanoparticles in the range of 9–20 nm size were obtained by the Scherrer equation using FWHM (Full Width at Half Maximum) values of the main peaks in the XRD diffraction pattern when calcined at 500 °C.

The UV–Vis–spectroscopy analyses have shown that all the thin films were transparent in the visible region with an average transmittance ranging from 70% to 87%. And showed a direct band gap reducing with increase in Fe^{3+} doping from 3.82 to 3.72 eV.

AFM images shown thin films with different contents of Fe. The effect of Fe concentration has been discussed.

Keywords: Thin films · SnO$_2$ oxide · Fe doped Sn · Optical analysis
AFM analysis

1 Introduction

Transparent conductive oxides (TCO) materials have been widely studied in recent years due to their optical and electrical properties such as: In$_2$O$_3$, SnO$_2$, ZnO, Cd$_2$SnO$_4$, CdSnO$_2$.

To improve the electrical properties of these transparent oxides, scientists have resorted to incorporate the dopants in these latter.

Obtaining such materials having a good compromise between transparency to visible light and good electrical conductivity, is a major industrial challenge.

Among these TCO materials tin dioxide (SnO$_2$) is the first transparent conductor commercialized abundantly, and an important semiconductor which has wider band gap of 3.6 eV and much higher exciton binding energy of 130 meV (Demichelis et al. 1984).

Due to its properties such as low electrical resistivity, high optical transmittance and high reflectivity in the infrared region, it can be used as anode in flat panel displays (Kotz et al. 1991). It is also one of the most metal oxides used in the control of air pollution and toxic gas detection (Takahata et al. 1988), as a conductive electrode in the thin film photovoltaic cells (Shang et al. 2012) and as a heat reflector in solar applications (Fukano et al. 2005). Sol-gel dip coating is employed to prepare thin films; this method is suitable to prepare homogenous layers with different doping.

In the present work we report the process for preparation of pure and Fe doped SnO$_2$ thin films from SnCl$_2$·2H$_2$O and FeCl$_3$ solutions by sol-gel dip coating method. The effect of Fe dopant on structural, morphological and optical properties of SnO$_2$ thin films has been studied.

2   Experimental

The samples were prepared by sol-gel technique using dip coating apparatus. As a starting material and dopant source, tin (II) chloride dihydrate (SnCl$_2$.2H$_2$O) and iron III chloride (FeCl$_3$·6H$_2$O). Firstly SnCl$_2$.2H$_2$O (2.5 g) was dissolved into 30 ml of absolute ethanol, then the solution, which was heated to 70 °C previously, was stirred by a magnetic stirring apparatus for 2 h.

Fe doped SnO$_2$ films have been prepared by adding an appropriate amount (1%, 2%, 3%, 5% and 10%) of FeCl$_3$·6H$_2$O to SnCl$_2$·2H$_2$O and dissolved by ethanol.

The obtained solution was continuously stirred for 2 h. Then the two solutions were stirred and heated at 70 °C for another 2 h. Finally, both mixtures were separately aged for 24 h at room temperature, a clear and homogeneous solutions was obtained.

The cleaned glass substrates were immersed in these solutions and withdrawn at the rate of 4 cm/min. The deposited films was then dried at 200 °C and finally annealed at temperature of 500 °C for 60 min. The procedures from coating to drying were repeated 10 times.

The Xray- diffraction patterns of samples were recorded by an X-ray diffractometer D6 Advance Bruker system using Cu Kα radiation (Cu Kα = 0.15406). The optical properties of the films were studied using A Jasko V-630 visible spectrophotometer. Atomic force microscope (AFM) measurements were carried out using A100-AFM microscopy.

3   Results and Discussion

3.1   X-Ray Diffraction Studies

To verify the crystallinity, we present the diffraction pattern of Fe doped SnO$_2$ thin layers after annealing of 500 °C.

Figure 1 shows peaks at $2\theta = 26.7°$, $34.8°$, $38.14°$. $51.55°$, $53.25°$ and $66.96°$ respectively correspond to the crystalline planes of SnO_2 rutile phase (110), (101), (200), (211), (220) and (301). Peak positions obtained are in good agreement with the tetragonal rutile structure of SnO_2 (Patil et al. 2012).
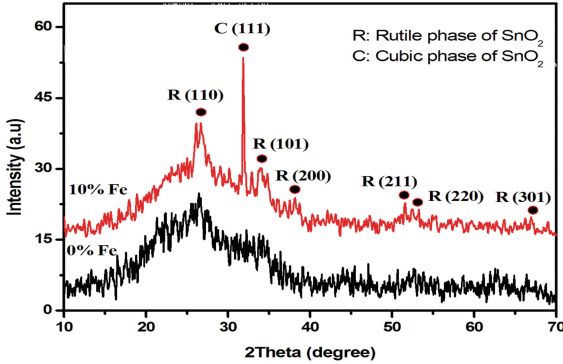

Fig. 1. XRD pattern of undoped and 10% Fe doped SnO_2 thin films.

The spectrum also shows a peak located at $2\theta = 31.88°$ assigned to the cubic phase (111) of SnO_2. The appearance of the cubic phase in the literature (Haines and Leger 1997) confirms our result and the reason to get it is due to the method followed and the materials used.

Moreover, no metallic iron phase, iron oxide or other phases were detected, which means a good dilution of the iron atoms in the SnO_2 structure in the XRD detection limits (Junbo et al. 2005).

The grain size (D) is calculated using the Debye-Scherrer formula (Patil et al. 2012):

$$D = \frac{0 \cdot 9\lambda}{\beta \cos \theta} \tag{1}$$

Where $\lambda = 0.154056$ nm is X-ray wavelength, β is FWHM, θ is Bragg's angle in degrees.

Figure 2 shows the width at half maximum (β) of 10% Fe doped SnO_2 and diffraction angle attributed to (211) peak.

The grain sizes are: 33.00; 48.39; 37.46; 38.74; 54.03 and 35.58 nm, respectively corresponding to the planes (110), (101), (200), (211), (220) and (301).
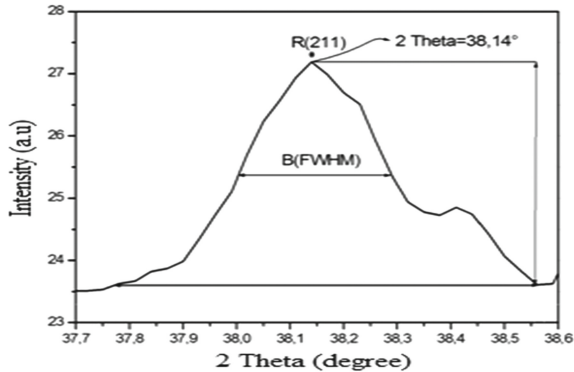
Fig. 2. Determination of the grain size from the measurement of FWHM (β) by the Debye Scherrer.

3.2   Surface Morphology Studies

Figure 3 shows AFM images in 2D and measurements of the roughness of pure and iron doped SnO$_2$ doped oxide layers deposited on glass substrates.
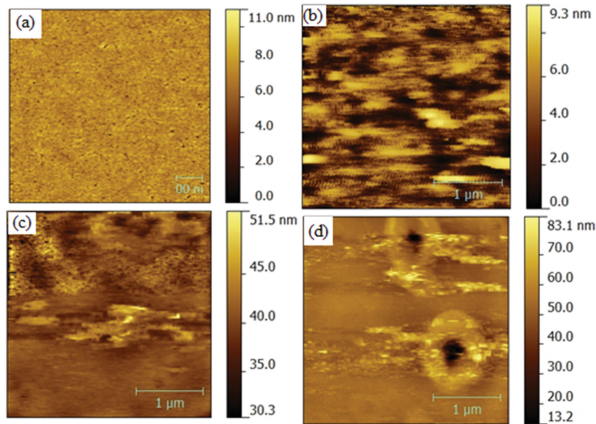

Fig. 3.   AFM images in 2D of SnO$_2$ thin films with different concentrations of Fe: (a) pure SnO$_2$, (b) 1% Fe-SnO$_2$, (c) 3% Fe-SnO$_2$ and (d) 5% Fe-SnO$_2$.

These images reveals that the gains are aleatory distributed throughout the sample surface, these surfaces are not rough enough. We can also be observed a small change of the grain size as a function of doping.

Pure SnO$_2$ is a spherical-shaped structure; the average grain size is 19 nm, whereas the root mean square (RMS) roughness is 27.28 nm. However, its topography changed following the introduction of Fe.

The average grain size was reported in Table 1 which decreases for 1% Fe and 5% Fe but increases to 20 nm for 3%. Fe The decrease in grain size can be attributed to the growing competition between the Fe phases and SnO_2 phases when the Fe concentration increases (Sakuma et al. 2007).

Table 1 summarizes the principal characteristics deduced from AFM images.

Table 1. The analytical data of AFM images

	Average size (nm)	Roughness (RMS) (nm)	Grain number
Pure SnO_2	19	27.28 ± 11.32	141
1% Fe	14.2	2.15 ± 1.12	77
3% Fe	20.5	4.83 ± 4.39	57
5% Fe	15.7	7.5 ± 2.21	71

3.3   Optical Properties

Figure 4 shows the optical transmission spectra of Fe doped SnO_2 films elaborated with different concentrations. It can be seen in this figure the presence of a good transparency region between 200 and 800 nm. The transmission is estimated at 60 to 90% in the visible which is strongly influenced by the doping, leading to a decrease in transmittance for 1% and 3% of Fe, and then rises again for 5% and 10% Fe reaching almost 90%.
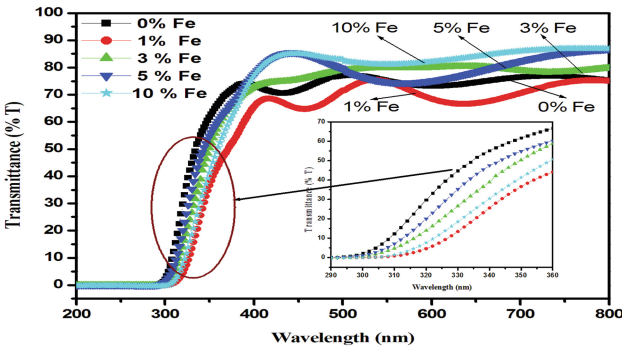

Fig. 4. Transmittance spectra of 0, 1, 3, and 5 mol% Fe, in SnO_2:Fe thin films.

We also note that the doped layer by 1% Fe has the smallest transparency in the visible. In fact, we observed a small shift of the absorption threshold towards higher energy with increasing doping.

Figure 4 also indicates that the doped films with 1% and 5% have more oscillations interference with respect to the other, indicating an increase in the film thickness (Khodja et al. 2014; Martinez et al. 2012).

The energy of the band gap is derived by the Tauc formula (Pankove 1971):

$$(\alpha h\upsilon)^2 = A\left(h\upsilon - E_g\right) \tag{2}$$

Where α, Eg and hν are: the absorption coefficient, the energy gap and the optical beam energy, respectively and A is a constant.

On Fig. 5 we represented the curves $(\alpha h\upsilon)^2$ for SnO$_2$ doped with different concentrations of iron.
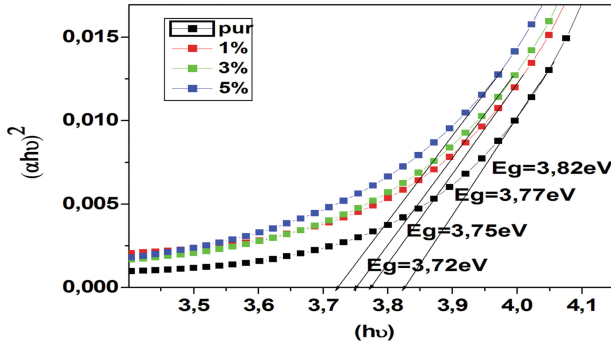

Fig. 5. Plot of $(\alpha h\upsilon)^2$ vs. photon energy of undoped and Fe-doped SnO$_2$ films.

As observed, the optical gap of the films is decreased when the concentration of Fe increases. The variation in the optical gap can be explained by the distortions in the crystal lattice of SnO$_2$ after the introduction of impurities that lead to the formation of the tail band in the band gap (Shajira et al. 2014).

4 Conclusions

The structural, morphological, optical and electrical thin layers of pure tin oxide doped with iron according to the synthesis conditions were studied in this work.

The X-ray spectrum of the SnO$_2$ thin films shows the formation of the crystalline structure after thermal annealing of 500 °C with great predominance of rutile nanoparticles. The grain size calculated from the Scherrer formula, vary between 33 and 54 nm according to the conditions of elaboration.

The morphological properties were examined by the AFM images, which show a aleatory distribution of gains on some samples. The surfaces are not sufficiently rough. The average grain size ranges between 14.2 and 20.5 nm and the roughness factor (RMS) varies between 7.5 and 27.28 nm.

Characterization of thin films developed by UV-Visible spectrophotometer showed a visible transmission is over 90% for the samples doped with 10% of Fe. Optical gap values vary between 3.72 and 3.82 eV.

References

Demichelis, F., Minetti-Mezzetti, E., Tagliaferro, A., Tresso, E.: Determination of optical properties of SnO_2 films. In: II Nuovo Cimento D, vol. 4, pp. 68–78 (1984)

Kotz, R., Stucki, S., Carcer, B.: Electrochemical waste water treatment using high overvoltage anodes. Part1: Physical and electrochemical properties of SnO_2 anodes. J. Appl. Electrochem. **21**, 14–20 (1991)

Takahata, K.: Tin dioxide sensors development and applications. Chem. Sens. Technol. **1**, 39–55 (1988)

Shang, G., Wu, J., Huang, M., Lin, J., Lan, Z., Huang, Y., Fan, L.: Facile synthesis of mesoporous tin oxide spheres and their applications in dye-sensitized solar cells. J. Phys. Chem. C **116**(38), 20140–20145 (2012)

Fukano, T., Motohiro, T., Ida, T., Hashizume, H.: Ionization potentials of transparent conductive indium tin oxide films covered with a single layer of fluorine-doped tin oxide nanoparticles grown by spray pyrolysis deposition. J. Appl. Phys. **97**, 084314 (2005)

Patil, G.E., Kajale, D.D., Gaikwad, V.B., Jain, G.H.: Preparation and characterization of SnO_2 nanoparticles by hydrothermal route. Int. Nano Lett. **2**, 17 (2012)

Haines, J., Leger, J.M.: X-ray diffraction study of the phase transitions and structural evolution of tin dioxide at high pressure: relationships between structure types and implications for other rutile-type dioxides. Phys. Rev. B **55**, 11144 (1997)

Junbo, W., Ming, Y., Yingmin, L., Licheng, C., Yan, Z., Bingjun, D.: Synthesis of Fe-doped nanosized SnO_2 powders by chemical co-precipitation method. J. Non-Cryst. Solids **351**, 228–232 (2005)

Sakuma, J., Nomura, K., Barrero, C., Takeda, M.: Mössbauer studies and magnetic properties of SnO_2 doped with 57Fe. Thin Solid Films **515**, 8653–8655 (2007)

Khodja, S., Touam, T., Chelouche, A., Boudjouan, F.: Effects of stabilizer ratio on structural, morphological, optical and waveguide properties of ZnO nano-structured thin films by a sol–gel process. Superlattices Microstruct. **75**, 485–495 (2014)

Martinez, D.Y.T., Perez, R.C., Delgado, G.T., Angel, O.Z.: Structural, morphological, optical and photocatalytic characterization of $ZnO–SnO_2$ thin films prepared by the sol–gel technique. J. Photochem. Photobiol. A Chem. **235**, 49–55 (2012)

Pankove, J.I.: Optical Processes in Semiconductors. Prentice-Hall Inc., Englewoord Cliffs (1971)

Shajira, P.S., Junaid Bushiri, M., Nair, B.B., Ganesh Chandra, P.V.: Energy band structure investigation of blue and green light emitting Mg doped SnO_2 nanostructures synthesized by combustion method. J. Lumin. **145**, 425–429 (2014)